Magnetic structure and electric field effects in multiferroic YMn_{2}O_{5}

R. A. de Souza, U. Staub, V. Scagnoli, M. Garganourakis, Y. Bodenthin, S.-W. Huang, M. García-Fernández, S. Ji, S.-H. Lee, S. Park, and S.-W. Cheong

Phys. Rev. B **84**, 104416 — Published 9 September 2011

DOI: 10.1103/PhysRevB.84.104416

Magnetic structure and electric field effects in multiferroic YMn_2O_5

R. A. de Souza,[1] U. Staub,[1] V. Scagnoli,[1] M. Garganourakis,[1] Y. Bodenthin,[1] S.-W. Huang,[1] M. García-Fernández,[2] S. Ji,[3] S.-H. Lee,[3] S. Park,[4] and S-W. Cheong[4]

[1] *Swiss Light Source, Paul Scherrer Institut, 5232 Villigen PSI, Switzerland*

[2] *Institut de Physique, Université de Fribourg, CH-1700 Fribourg, Switzerland*

[3] *University of Virginia / NIST, Center for Neutron Research, Gaithersburg, Maryland 20899, USA*

[4] *Rutgers Center for Emergent Materials and Department of Physics and Astronomy, Rutgers University, Piscataway, New Jersey 08854, USA*

(Dated: August 5, 2011)

The magnetic structure of multiferroic RMn_2O_5 (R=Y,Er) has been investigated by means of resonant soft x-ray diffraction. Energy, temperature and azimuthal angle scans were performed in addition to reciprocal space maps on the magnetic reflection in the different magnetic phases of YMn_2O_5. We also investigated the orbital magnetic moment at the oxygen K-edge for RMn_2O_5 with both, R= Y and Er compositions. These moments reflect the strong hybridization between Mn 3d and oxygen 2p states. Experiments with applied electric fields are additionally presented, showing that the helical component of the magnetic structure in the CM phase of YMn_2O_5 can be reversed by the application of an electric field. However, the incommensurate magnetic reflection in the high temperature phase is unaffected. Interestingly, this is observed only in the presence of a small electrical current, indicative of a current induced/enhanced switching of magnetic domains.

PACS numbers: 75.25.-j, 78.70.Ck

I. INTRODUCTION

The interest for multiferroic materials, in which electric polarization coexists with magnetic order, has strongly increased in the last decade. Especially interesting, for technological application in spintronic devices, are materials where there is a strong coupling between magnetism and ferroelectricity. This magnetoelectric coupling is observed in systems with frustrated magnetic interactions such as the $RMnO_3$ and RMn_2O_5 families (R=rare-earth ion).[1,2] Due to this gigantic coupling, the application of magnetic fields affects strongly the ferroelectric properties. Even more interesting is to alter the magnetic properties by the application of an electric field.[3–8] For example, the application of an electric field during cooling through the ferroelectric transition allows to select a single defined spin helicity of the spiral magnetic structure in $TbMnO_3$.[6,9] Strong electric fields perpendicular to the ferroelectric polarization affect the commensurate magnetic structure in $ErMn_2O_5$. This is observed through induced intensity of the commensurate magnetic $(\frac{1}{2}\ 0\ \frac{1}{4})$ reflection. An hysteretic behavior of the intensity versus applied electric field is additionally observed.[7]

The RMn_2O_5 family presents a variety of magnetic phases with complex incommensurate and noncollinear commensurate phases. The magnetic phase diagram can be separated into three or four regions depending on the rare-earth.[10,11] Below T_N, the system first enters a 2D incommensurate (HT-ICM) phase, which is characterized by a wave vector $\mathbf{q} = (q_x\ 0\ q_z)$. On further cooling the magnetic structure will lock in either a 1D incommensurate phase (1D-ICM) with $\mathbf{q} = (q_x\ 0\ \frac{1}{4})$, depending on the rare-earth, or directly transform to the commensurate state (CM), where $\mathbf{q} = (\frac{1}{2}\ 0\ \frac{1}{4})$. At lower temperatures, a different incommensurate phase appears (LT-ICM) with $\mathbf{q} = (q_{x2}\ 0\ q_{z2})$. For YMn_2O_5 the HT-ICM, CM and LT-ICM transitions occur at $T_N = 45$ K, $T_{C1} = 39$ K, and $T_{C2} = 19$K, respectively.[10] The 1D-ICM exists only in a small range of approximately 1 K around T_{C1}.[12]

The complex magnetic structure of CM and LT-ICM phase of YMn_2O_5 has been revised by Kim et al. combining four-circle and polarized neutron diffraction.[13] They show that in the CM structure, there are two types of cycloidal spirals along the c-axis. In addition, their model shows that the Mn^{3+} and Mn^{4+} moments form a zigzag chain in the *ab* plane, with moments being nearly collinear. The CM phase presents a net polarization along the *b* axis, which is induced by the magnetic structure. The LT-ICM phase of YMn_2O_5 presents complex spiral structures along the *a* and *c* axes.[13] The spirals in the *bc* plane are no longer in phase which is proposed to reduce the net polarization. Such a weakening of the ferroelectric polarization at lower temperature has been observed experimentally.[14] However, because of the complexity of the magnetic structure usually present in these compounds, the underlying mechanism of multiferroicity is still under discussion.[13,15,16]

Resonant x-ray scattering has become a powerful technique to study magnetic and electronic ordering phenomena and has been applied to different compounds of the RMn_2O_5 family.[7,17–23] The soft x-ray range has the advantage to directly probe the $3d$ Mn and $4f$ R states using the $L_{2,3}$ and the $M_{4,5}$ edge resonances, respectively. Such technique has been previously used to study the Er[7,18] and Tb[20–22] compounds of the RMn_2O_5 series. Despite these intense studies, some questions remain open. One of them regard the interplay between the magnetic moments of manganese and the rare-earth in these compounds. An additional important question concerns the role of exchange striction versus the spirals concerning the origin of the magnetoelectric coupling. Recently, it has been shown that the induced magnetic moments at the oxygen might be important to understand the multiferroicity in these materials.[21,24] Resonant x-ray diffraction is an elemental sensitive technique that can probe the magnetism of the different elements separately, but information on the different ions is still missing. Another important aspect to understand multiferroics is the interplay between electric fields and the magnetic order, as this represents the magnetoelectric coupling directly. To date, resonant x-ray diffraction under applied electric field observing a change in magnetism has only been applied to $ErMn_2O_5$[7] and very recently to $TbMnO_3$[25]. In the latter, a different domain population was observed by cooling in electric fields. To address these open points we used resonant soft x-ray diffraction to study the magnetic structure in the different phases in YMn_2O_5, including application of electric fields.

This paper is structured as follows. After the experimental section, the presented results are split into studies of the temperature evolution of the magnetic order (A), the spectral dependence of the magnetic reflection (B), the azimuthal angle dependence of the reflection (C), and finally into the effects of applied electric fields on the magnetic structure (D). These issues are then discussed and the conclusions are presented.

II. EXPERIMENT

Single crystals of YMn_2O_5 were grown using $B_2O_3/PbO/PbF_2$ flux in a Pt crucible, as described elsewhere.[26] The crystals have been characterized with Cu Kα radiation. They were oriented and cut to have the [2 0 1] direction

normal to the surface. Resonant soft x-ray diffraction experiments have been performed at the RESOXS[27] endstation at the SIM[28] beamline of the Swiss Light Source at the Paul Scherrer Institut. Measurements were carried out in horizontal scattering geometry at the Mn $L_{2,3}$ and O K edges. The sample was cooled to temperatures between 10 and 60 K using a helium-flow cryostat. The linear polarization of the incident radiation was either horizontal (π), parallel to the scattering plane, or vertical (σ), perpendicular to the scattering plane. Polarization analysis of the scattered radiation was performed using a graded W/C multilayer setup.[27,29] Rotations around the Bragg wave vector (azimuthal angle Ψ) used the rotatable sample transfer fork with accuracy better than five degrees. An azimuthal angle of zero degrees ($\Psi = 0°$) reflects the situation of [0 1 0] direction perpendicular to the horizontal scattering plane. Electric field has been applied parallel to the b-axis in situ, and measurements were performed with either right- or left-handed circular polarization at $\Psi = 0$.

III. RESULTS

A. Temperature dependence

In order to follow the different magnetic phases present in YMn_2O_5, we scanned the reciprocal space and collected the scattered intensity for different temperatures. These reciprocal space maps, measured with the sample at $\Psi = 0$, are shown in fig. 1. In the low temperature phase (fig. 1(a)), at T=10K, two reflections are observed. One of them corresponds to the commensurate phase (CM) phase with $\mathbf{q} = (\frac{1}{2}\ 0\ \frac{1}{4})$. The second reflection can be attributed to the low temperature incommensurate phase (LT-ICM), with propagation vector $(\frac{1}{2} + \delta_x\ \ 0\ \ \frac{1}{4} + \delta_z)$ with $\delta_x = 0.012$ and $\delta_z = 0.03$. The fact that both reflections are observed are observed simultaneously indicates the first order character of this phase transition. The propagation wave vector determined by neutron diffraction are very close to the modulus of the values of δ_x and δ_z obtained here.[12,13] It is interesting to note that the commensurate peak is more diffuse along $[h\ 0\ \frac{1}{4}]$ than the LT-ICM one, which is almost isotropic. Such a coexistence of CM and LT-ICM phases has been previously observed in other RMn_2O_5 compounds (R=Dy,Er and Ho).[17,30,31]

In the CM phase, T=22 K (fig. 1(b)), the peak presents more extended tails of diffuse scattering. Here we observe again diffuse scattering along $[h\ 0\ \frac{1}{4}]$ and interestingly also parallel and almost perpendicular to ordering wave vector $\mathbf{q}$ in the plane with $k = 0$. Similar diffuse scattering has been previously observed in $ErMn_2O_5$.[18] One also notes the small, but distinguishable, intensity still present at the position of the LT-ICM one. This diffuse anisotropic scattering represents directions with less perfect magnetic order (correlations), which show the frustrated character of the magnetic exchange interactions.

At T=39.5 K (fig. 1(c)) the commensurate peak splits into two reflections of type $(\frac{1}{2} \pm \delta_x\ 0\ \frac{1}{4})$, with $\delta_x = 0.0125$ and the reflection with $h = \frac{1}{2} - \delta_x$ is much weaker than that of $h = \frac{1}{2} + \delta_x$. The system is in the 1D-ICM phase, which is present only in approximately 1 K temperature range. In fact, partial maps (not shown) at intermediate temperatures show the peak becoming elongated along h before it really splits. Clear diffuse scattering along h is already visible at 22K (fig.1(b)). In the 1D-ICM phase, the diffuse scattering along $[h\ 0\ \frac{1}{4}]$ is still present, and there is also diffuse scattering perpendicular to this direction, along $[\frac{1}{2} + \delta_x\ 0\ l]$.

At T=40.5 K (fig. 1(d)) the two peaks move away from the commensurate l position, entering the HT-ICM phase with $(\frac{1}{2} \pm \delta_x\ \ 0\ \ \frac{1}{4} + \delta_z)$, and they become further apart from each other, with $\delta_x = 0.015$ and $\delta_z = 0.006$. The reflection $(\frac{1}{2} + \delta_x\ \ 0\ \ \frac{1}{4} + \delta_z)$ is still diffuse along l, but no longer along h. These changes in the directional diffuse scattering across the phase transitions are indicative of the competing interactions in this complex magnetic structure.

B. Energy dependence

The energy dependence of the magnetic reflections around the Mn $L_{2,3}$ edges is presented in fig. 2. The corresponding magnetic phases are indicated in the figure. Measurements with π and σ incident x-ray polarization are presented in each phase. All the different phases present the same basic features, the spectra are composed of three main peaks, labeled A (641.1 eV), B (644.1 eV) and C (652.7 eV) in the figure. The relative intensity of these three different features varies with temperature, even in the commensurate phase ($22K \leq T \leq 37K$). These intensity ratio variations in the CM phase point to changes of the magnetic structure with temperature within this phase. These changes might reflect the different contributions of the magnetic moments from the Mn^{3+} and Mn^{4+} ions, caused

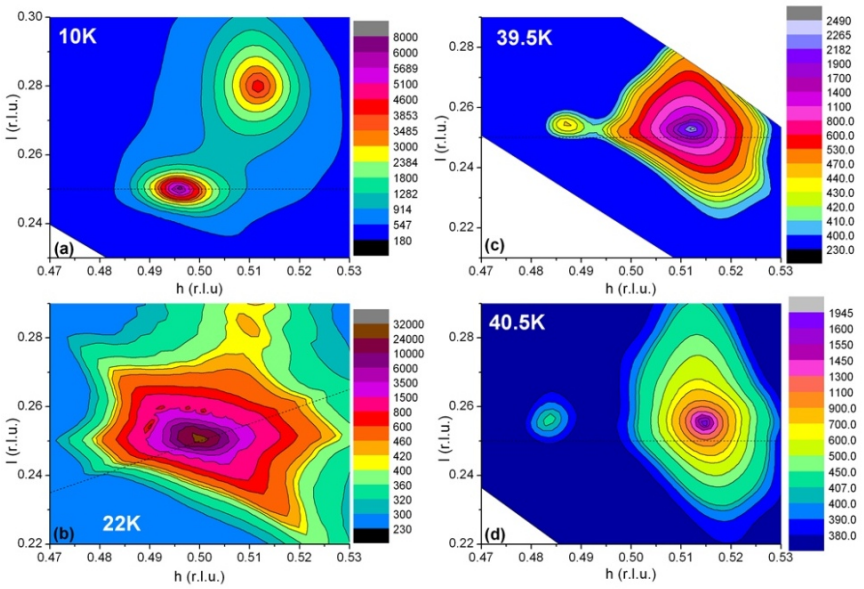

Figure 1. X-ray intensity maps in reciprocal space around the position ($\frac{1}{2}$ 0 $\frac{1}{4}$), collected at the Mn L_3 edge (644.1 eV) with π incident polarization at $\Psi = 0°$ (**b** perpendicular to the scattering plane). The temperature of each map is indicated. The solid line in (a),(c) and (d) indicate the commensurate l=0.25 position, while in (b) it represents the [$\frac{1}{2}$ 0 $\frac{1}{4}$] direction

by a rotation of these moments with the change in temperature. However, this does not necessarily mean that the modulus of these moments have a different temperature dependence. It may indicate that the individual moments change their direction in addition to their value, and correspondingly contribute differently to the structure factor of the observed reflection. Evidences of such a change in the magnetic structure inside the CM phase have also been observed in $ErMn_2O_5$,[18] and seem to be common for the RMn_2O_5 series.

The energy dependence measured in the CM phase at different azimuthal angles is presented in fig. 3. Once more, the relative intensity between the different features is different at the different Ψ positions. The complex CM phase determined by Kim et al.[13] is composed of different spiral and zigzag chains formed by the Mn^{3+} and Mn^{4+} moment components along the different directions. These components probably lead to different contributions to the energy scans, and these contributions will not be the same at the different azimuths.

A recent resonant soft x-ray scattering study on $TbMn_2O_5$ found an antiferromagnetic spin polarization at the oxygen sites.[21] Here we have checked for such spin polarization in both Y and Er compounds (RMn_2O_5, R=Y,Er) by measuring the commensurate magnetic reflection ($\frac{1}{2}$ 0 $\frac{1}{4}$) at the O K-edge. A clear signal is observed for both compounds, as can be observed in fig. 4. The fluorescence background has been subtracted in the spectra shown in fig. 4 (a) and (b). The inset shows the energy scan obtained by **q** scans for each energy point, measured with σ incident polarization, for comparison. The shape of the energy scans measured with π and σ incident light is similar, with a main peak around 529.5 eV (M) and a smaller feature (P) at higher energy. The intensity is much weaker for σ incident polarization. It is also interesting that the intensity ratio between I_π/I_σ at the two spectral features is different between the R=Er and Y case.

C. Azimuthal angle dependence

The azimuthal angle (Ψ) dependence of the commensurate reflection ($\frac{1}{2}$ 0 $\frac{1}{4}$) in YMn_2O_5 measured at feature **B**, the strongest spectral feature of the energy scan (see fig. 2), is presented in fig. 5 for π and σ incident polarization. It is similar to the one observed for $ErMn_2O_5$,[18] with an extended low intensity region observed in the σ channel for $-60° < \Psi < 50°$ and a maximum at $\Psi = 180°$, where the intensity in the π channel is minimum. It also shows a double peak in the π channel around $\Psi = 0$.

The variation of the diffraction amplitude in an azimuthal scan at resonance is given in the electric-electric dipole

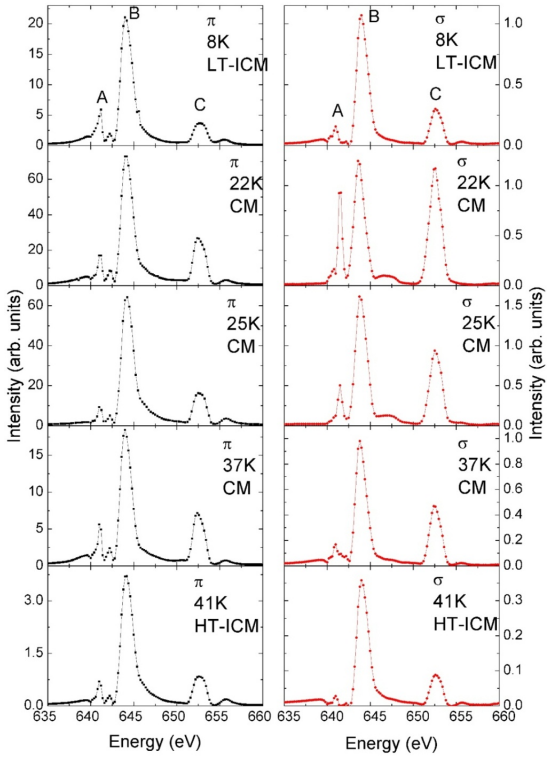

Figure 2. Energy scan of the magnetic reflection at different temperatures. The different phases measured are identified in the picture. The wave vectors correspond to $(\frac{1}{2}+\delta_x \;\; 0 \;\; \frac{1}{4}+\delta_z)$ with $\delta_x = 0.012$ and $\delta_z = 0.03$ at 8K (LT-ICM), $(\frac{1}{2}\;0\;\frac{1}{4})$ for $22K \leq T \leq 37K$ (CM), and $(\frac{1}{2}+\delta_x\;0\;\frac{1}{4}+\delta_z)$ with $\delta_x = 0.015$ and $\delta_z = 0.006$ at 41 K (HT-ICM). Measurements with π and σ incident x-ray polarizations in each case, with sample at $\Psi = 0^\circ$.

transition as:

$$F(\theta) = \sum_{Kq}(-1)^q \mathbf{X}^K_{-q}(\theta) \sum_{q'} D^K_{q'q}(\gamma_0, \beta_0, \alpha_0) \mathbf{\Psi}^K_{q'} \tag{1}$$

The angles $\alpha_0, \beta_0, \gamma_0$ are related to the Euler angles of the rotation that aligns the Bragg vector τ along the a-axis. $\mathbf{\Psi}^K_q$ is the tensor associated with the electrons and is given by the expression $\mathbf{\Psi}^K_q = \sum_d \left\langle \mathbf{T}^K_q \right\rangle e^{i\mathbf{Q}.\mathbf{d}}$, in which the sum over d runs over all the resonant ions in the unit cell, and where $\mathbf{d}$ is the position of the ions within the unit cell. $D^K_{q'q}(\gamma_0, \beta_0, \alpha_0)$ are the Wigner functions that correspond to the matrix elements of the rotations in the angular momentum representation[32] and K is the rank of the tensor. A tensor of rank $K = 1$ represents the origin of magnetic scattering. A general model not specifying further the magnetic structure with ordering wave vector $(\frac{1}{2}\;0\;\frac{1}{4})$, as applied for the interpretation of a magnetic reflection of the layered cobaltate,[33] is used. Here we describe the σ and π incident polarization scans separately and not their ratio. Since they show clear minima with intensities close to zero, the ratio thus is not an appropriate quantity for the analysis.

The expression $\mathbf{\Psi}^K_{\pm q}$ reflects the sum of the magnetic moment components along the different axis weighted by the crystallographic phase factor: $\mathbf{\Psi}^1_0 \equiv m_z$, $\mathbf{\Psi}^1_x = \frac{1}{\sqrt{2}}(\Psi^1_{-1} - \Psi^1_{+1}) \propto m_x$, and $\mathbf{\Psi}^1_y = \frac{i}{\sqrt{2}}(\Psi^1_{-1} + \Psi^1_{+1}) \propto m_y$. A fit to the parameters m_x, m_y and m_z, as done for $ErMn_2O_5$,[18] is presented in fig. 5. But contrary to the results observed for the Er compound, the fit describes the azimuthal angle dependence pretty well in the present case. The fit results in values of $m_x \approx -m_y$ and $m_z \approx 0$. The value $m_z \approx 0$ does not necessarily imply that all the individual z components of the Mn moments are zero. Nevertheless, it directly shows that the assumption made by Okamoto et al.[20] on the z component of $S_q = \sum_d \vec{S}_d \, e^{i\mathbf{Q}.\mathbf{d}}$, with $\vec{S}_d$ being spin moments of the ion with position $\mathbf{d}$, would apply better in the Y compound than in the Er case. The Er ions are supposed to induce a significant z component on the individual magnetic Mn moments. Such components were observed by neutron diffraction.[34] It would be interesting to know if such a model would be applicable for the $TbMn_2O_5$, since Tb may also induce some magnetic moments. Beale et al.[21] have measured the azimuthal angle dependence at the Mn L_3 edge, but only in a limited range, and it is not easy to make a comparison to the data in Er[18] and Y compounds.

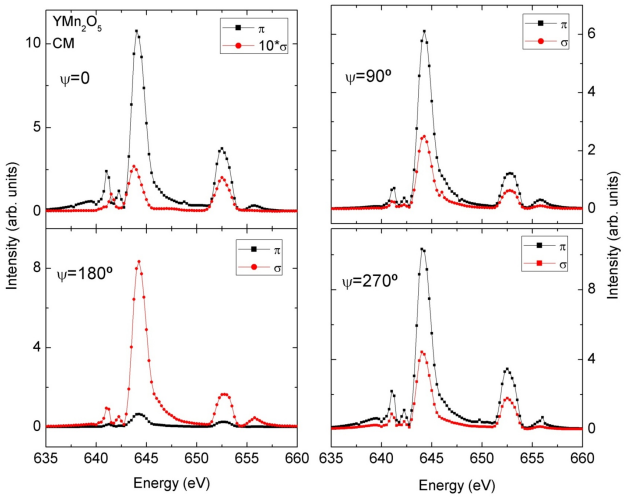

Figure 3. Energy scan of the commensurate magnetic reflection $(\frac{1}{2}\ 0\ \frac{1}{4})$ at different azimuthal angles (Ψ) measured with π and σ incident polarization. Measurements done at 25K.

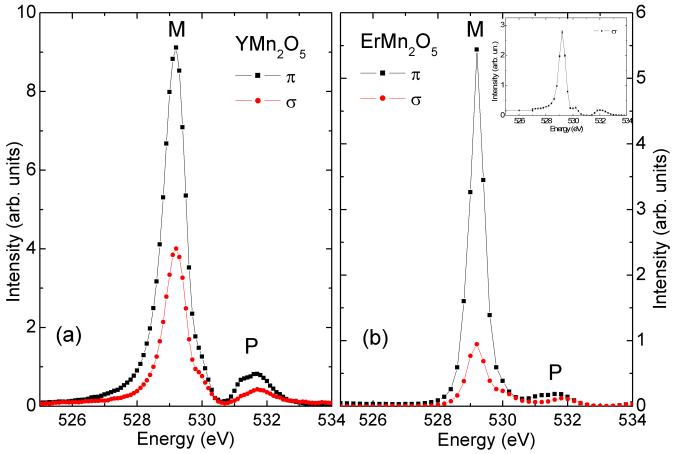

Figure 4. (a) Energy scan of the $(\frac{1}{2}\ 0\ \frac{1}{4})$ reflection of YMn_2O_5 (a) and $ErMn_2O_5$ (b) around the O K-edge. The fluorescence background has been substracted. Measurements with π and σ incident polarization in each case. Inset: Energy scan of $ErMn_2O_5$ obtained with $\theta/2\theta$ scans at each energy.

Though the description of the azimuthal angle dependence with this general model is accurate and the agreement with the data excellent, the assignment of the function to the individual moments sizes, respectively their weighted directional structure factor components is not necessarily a good approximation. The limitations are twofold. First, the mixture of the Mn^{3+} and Mn^{4+} moments have a different resonant strength at the edge. Secondly, the different directions of the moments can also have a different spectral shape (strength) as e.g. observed by XMCD.[35] In other words, looking at the general model introduced by Scagnoli and Lovesey,[36] the different tensors of rank one (being magnetic), will have different spectral shapes. This is primarily important for low symmetric systems, as it is the case for the RMn_2O_5 systems in the ferroelectric state. Both effects would lead to energy (spectral feature) dependent azimuthal angle scans, which is actually experimentally observed here. Therefore, qualitative values would have to be taken with some caution.

D. Electric field effect

To study the magnetoelectric interaction we performed in situ experiments with applied electric fields along the polar b-axis. For these experiments, the crystal was mounted with the b-axis perpendicular to the diffraction plane (vertical), what correspond to $\Psi = 0°$. An external electric field up to ±10 kV/cm was applied. The measurements used circular polarized light, and were performed in focus mode, with a $100\mu m$ beam size on the sample. Circular polarized x-rays are a powerful tool to study spiral magnetic structures, since they directly couple to the helicity of the magnetic structure.[9,25,37–39]

Without any applied electric field, the intensity of the diffraction peak with right (C+) and left (C-) handed circular polarized light was the same (fig. 6 (a)). So was it with applied electric fields up to ± 10 kV/cm without any current flowing through the sample. After the emission of a spark, current started flowing when an electric field was applied to the sample. In this case, the intensity measured with circular light of different helicity became inequivalent. In order to confirm the reproducibility of the effect, the following measurements were carried out.

First the sample was cooled from above T_N to 25K (in the CM phase) under applied electric field (FC) of -5 kV/cm. At this temperature, we have measured the diffraction peak with an applied electric field, using circularly polarized light. In fig. 6 ((b) and (c)) the measurements at approximately ±5 kV/cm are presented, showing a clear difference between C+ and C- intensity. In fact, two peaks are observed, which are labeled E and F in the figure. The first one (E), which corresponds to the CM phase, is strongly affected by the electric field. The second one (F) shows no dependence on circular light, and it corresponds to the 1D-ICM phase. This means that the sample is being significantly heated, with the applied fields of ± 5kV/cm, to a temperature close to phase transition between these two states, as peak F is absent in zero electric fields.

There are two possible sources for the heating, one is the x-ray beam, that in focus mode concentrate all the intensity in a very small spot. The second one is a small current flowing through the sample during the application of the electric field. The inset of fig. 6 also shows the intensity of the CM diffraction peak when increasing the field from -5 kV/cm until +5 kV/cm using circular polarized light. The field-cooled sample presents a difference in intensity

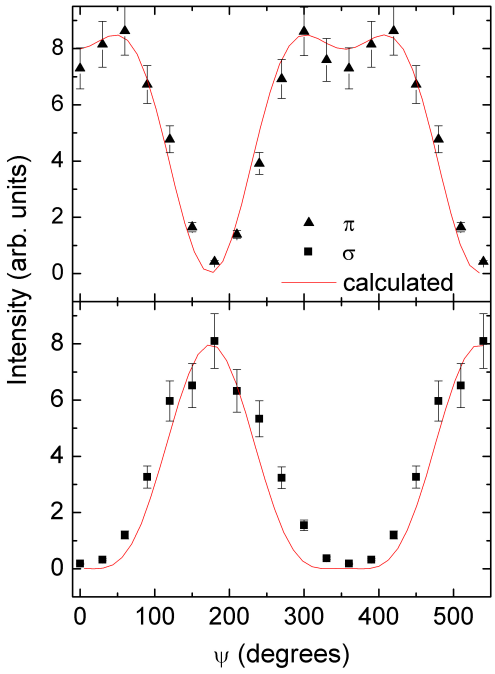

Figure 5. Azimuthal angle dependence of $(\frac{1}{2}\ 0\ \frac{1}{4})$ reflection of YMn_2O_5 measured at the Mn L_3-edge (644.1 eV) with π and σ incident polarization, at $\Psi = 0$, and fit to a general magnetic model. Measurements done at 25K. Data for $\Psi > 360°$ are replotted from low Ψ data (I(Ψ)=I($\Psi + 360°$)) for better visual.

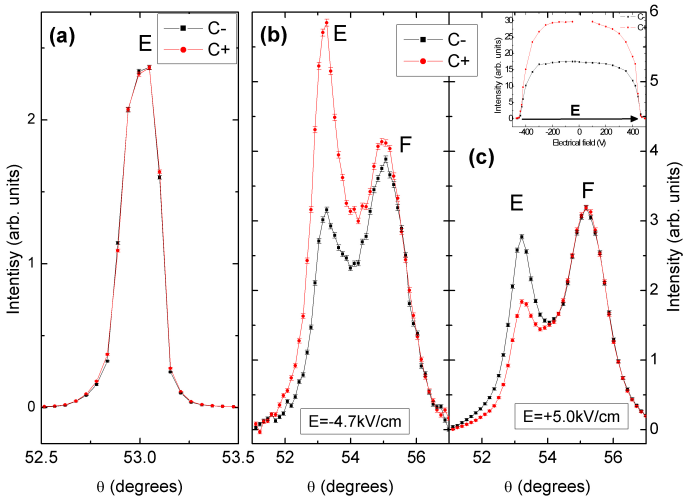

Figure 6. (a) Rocking curve of the CM peak measured at the Mn L_3 edge with right (C+) and left (C-) handed circularly polarized light, before applying electric field. $\theta/2\theta$ scans measured with C+ and C- polarized light at (b) -4.7 kV/cm and (c) +5.0 kV/cm applied field. E is the CM position and F is the 1D-ICM position. Inset: diffraction intensity measured at the commensurate $(\frac{1}{2}\ 0\ \frac{1}{4})$ position when increasing the field from -4.7 kV/cm to +5.0 kV/cm.

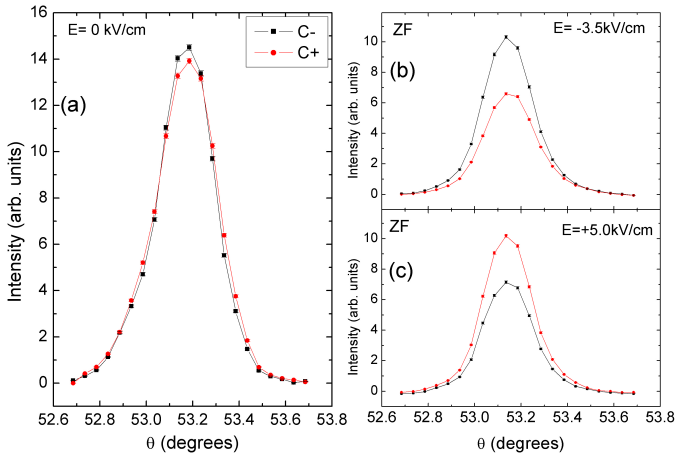

Figure 7. $\theta/2\theta$ scans measured with right (C+) and left (C-) handed circularly polarized light (a) before electric field was applied and after (b) -3.5 kV/cm and (c) +5.0 kV/cm applied field.

for C+ and C- polarization, even at zero field, in contrast to the sample in its initial state (see fig. 6 (a)) . Only above a certain threshold the intensity of C+ and C- is inverted in the CM phase. This means that the helicity of the CM cycloidal structure has been inverted by the applied electric field. Similar result has been observed by neutron polarimetry studies on the same compound.[8] The neutron study showed that when warming up the sample close enough to the phase transition, it was possible to change the magnetic domain population with an applied electric field. Here we confirm the inversion of the magnetic domains with different helicity in the ferroelectric CM phase. Additionally we show that the 1D-ICM phase is not affected by the electric field.

In a second step, in order to decrease the heat load in the sample and to study the CM phase alone, the intensity of the x-rays has been decreased by approximately one order of magnitude. For that only one of the two undulators and narrower front slits were used. The sample was cooled under zero field (ZFC) to lower temperature, around 10K (measured on the cold finger) in order to compensate for the extra heat produced by the current. The first measurements were done without electric fields. The results are shown in fig. 7(a). As in the initial state of the sample, without an applied field one observes no difference in the intensity measured with C+ or C-. This is also an indication that the spark did not permanently damaged or altered the sample. An electric field of 5 kV/cm, with

different polarity, was then applied for a few seconds alternatively. A current is concomitantly flowing through the sample during this time. The resulting zero field (ZF) scans are shown in fig. 7 (b and c). By the position of the peak, it is possible to affirm that the sample remains in the CM phase, as expected. The observed electric field effect is still present. The electric field pulse or current is sufficient to induce a change in the relative intensity measured with C+ and C- polarized x-rays. This indicates a change of the magnetic domain population with different helicity, by the application of the electric field/current.

IV. DISCUSSION

The smaller intensity ratio between the two spectral features (I_M/I_P) at the oxygen K-edge observed in $ErMn_2O_5$ in respect to the one observed in YMn_2O_5 suggests that the electronic states at the oxygen differs for the two compounds. This also indicates that the magnetic induced moment at oxygen is not solely caused by the Mn moments, but an interplay between Mn-O and Er-O couplings. The influence of the erbium magnetic moment in the magnetic structure could also be related to the unsatisfactory agreement of the observed azimuthal angle dependence with the general model in that compound.[18] Yttrium being non magnetic, such a contribution is absent in the present study on YMn_2O_5. This results in a much better modeling of the azimuthal angle dependence of the yttrium compound.

We have shown that the magnetic structure can be modified with an applied electric field/current in the CM phase, while it is unaffected in the 1D-ICM phase. This is an interesting observation in two aspects. Let us first discuss the absence of an electric field effect on the peak representing the 1D-ICM phase. This absence is in contrast with the general believe that the magnetic induced ferroelectricity is connected to the 1D-ICM phase. This means either that the 1D-ICM phase does not exist as separate phase or that it is not ferroelectric. Alternatively, the 1D-ICM phase could be ferroelectric, but there is no coupling to the helical component of the magnetic structure. The latter would indicate that the ferroelectricity is indeed exchange striction driven. It has also been shown that the electric field effect in $ErMn_2O_5$ is affecting mainly the commensurate magnetic reflection, with little or no changes to the 1D-ICM reflections.[7] Note that there, the electric field is applied perpendicular to the ferroelectric polarization, and the x-ray probe measures a change of magnetic structure, not a change of magnetic domain population, in contrast to the results presented here. Again that study indicates that the coupling of electric field affects mainly the CM phase. Investigations in the 1D-ICM phase temperature regime by neutron scattering are also contradictory. There are studies supporting the existence of the 1D-ICM phase[12] and studies supporting its absence.[40] The reciprocal space maps presented here (fig. 1) are not really conclusive on this issue either. They clearly show that the temperature dependence of ratio δ_x/δ_z is strongly non linear. However, this is not sufficient to prove the existence of the 1D-ICM phase. The same ambiguity exist in the interpretation of the published reciprocal space maps by resonant x-ray diffraction on $ErMn_2O_5$.[18]

Moreover, the presented results indicate that the size of the applied static electric fields is insufficient to switch the magnetic domains alone. The switching occurs only in the case when a current is flowing, and hence the applied electric fields are smaller. This might be related to the recent observation of the interaction of the x-ray beam with the domain formation of magnetic domains in $DyMnO_3$.[38] In that study, it was shown that the x-ray beam can trigger a domain wall of the different helical domains, probed through the Dy 4f moments. It is proposed that this is caused by the photoelectric effect. The emitted electrons do not only charge the material, but also create small currents and discharges, which might facilitate the domain formation. Such a scenario would be supported by our observation that the current affects the domain transformation much more than the static field. This view might also be corroborated by the observation of domain wall motions induced by currents in antiferromagnets.[41] Therefore, the electric current or current pulse might push the magnetic domain walls, which initiates the process of reversing the helicity of the magnetic spiral and consequently the electric polarization.

V. CONCLUSION

Resonant soft x-ray diffraction has been applied to study the magnetic structure of the Mn and O sublattice in multiferroic YMn_2O_5. In the Mn sublattice, the different azimuthal and temperature dependence of the energy spectra of the commensurate reflection ($\frac{1}{2}$ 0 $\frac{1}{4}$) is caused by individual spectral shapes of the magnetic Mn^{3+} and Mn^{4+} scattering factors. The azimuthal angle dependence of the commensurate magnetic reflection measured at the Mn L_3 edge can be accurately described solely by magnetic scattering from magnetic dipoles. A clear orbital magnetic moment is observed at the oxygen K-edge for RMn_2O_5, with both R=Y and Er. However the intensity ratio between

the different polarizations, π and σ, for the different spectral features differ in the two compounds. This is a clear indication that the Er-O (or Er-Mn) magnetic interaction is modifying the orbital state at the oxygen. The application of electric fields induces a reversal of the helical component of the commensurate magnetic structure in YMn_2O_5, while the high temperature 1D incommensurate phase remains unchanged. Moreover, this effect is only observed in the presence of a small electric current, which indicates a current assisted switching of the magnetic domains.

ACKNOWLEDGMENTS

We have benefited from the experimental support of the X11MA beamline staff. Financial support of the Swiss National Science Foundation and its NCCR MaNEP is gratefully acknowledged. Work at Rutgers was supported by DOE DE-FG02-07ER46382 and work at UVA was supported by the US NSF under Agreement No. DMR-0903977

[1] T. Kimura, G. T., H. Shintani, K. Ishizaka, T. Arima, and Y. Tokura, Nature (London) **426**, 55 (2003).
[2] N. Hur, S. Park, P. Sharma, J. Ahn, S. Guha, and S.-W. Cheong, Nature (London) **429**, 392 (2004).
[3] E. Ascher, H. Rieder, H. Schmid, and H. Stössel, J. Appl. Phys. **37**, 1404 (1966).
[4] T. Lottermoser, T. Lonkai, U. Amann, D. Hohlwein, J. Ihringer, and M. Fiebig, Nature (London) **430**, 541 (2004).
[5] T. Zhao, A. Scholl, F. Zavaliche, K. Lee, M. Barry, A. Doran, M. P. Cruz, Y. H. Chu, C. Ederer, N. A. Spaldin, R. R. Das, D. M. Kim, S. H. Baek, C. B. Eom, and R. Ramesh, Nature Mater. **5**, 823 (2006).
[6] Y. Yamasaki, H. Sagayama, T. Goto, M. Matsuura, K. Hirota, T. Arima, and Y. Tokura, Phys. Rev. Lett. **98**, 147204 (2007).
[7] Y. Bodenthin, , U. Staub, , M. Garcia-Fernandez, M. Janoschek, J. Schlappa, E. I. Golovenchits, V. A. Sanina, and S. G. Lushnikov, Phys. Rev. Lett. **100**, 027201 (2008).
[8] P. G. Radaelli, L. C. Chapon, A. Daoud-Aladine, C. Vecchini, P. J. Brown, T. Chatterji, S. Park, and S.-W. Cheong, Phys. Rev. Lett. **101**, 067205 (2008).
[9] F. Fabrizi, H. C. Walker, L. Paolasini, F. de Bergevin, A. T. Boothroyd, D. Prabhakaran, and D. F. McMorrow, Phys. Rev. Lett. **102**, 237205 (2009).
[10] H. Kimura, S. Kobayashi, Y. Fukuda, T. Osawa, Y. Kamada, y. Noda, I. Kagomiya, and K. Kohn, J. Phys. Soc. Jpn **76**, 074706 (2007).
[11] S. Kobayashi, T. Osawa, H. Kimura, and Y. Noda, J. Korean Phys. Soc. **46**, 289 (2005).
[12] S. Kobayashi, T. Osawa, H. Kimura, Y. Noda, I. Kagomiya, and K. Kohn, J. Phys. Soc. Jpn **73**, 1593 (2004).
[13] J.-H. Kim, S.-H. Lee, S. I. Park, M. Kenzelmann, A. B. Harris, J. Schefer, J.-H. Chung, C. F. Majkrzak, M. Takeda, S. Wakimoto, S. Y. Park, S.-W. Cheong, M. Matsuda, H. Kimura, Y. Noda, and K. Kakurai, Phys. Rev. B **78**, 245115 (2008).
[14] Y. Noda, Y. Fukuda, H. Kimura, I. Kagomiya, S. Matumoto, K. Kohn, T. Shobu, and N. Ikeda, J. Korean Phys. Soc. **42**, S1192 (2003).
[15] A. B. Harris, A. Aharony, and O. Entin-Wohlman, Phys. Rev. Lett. **100**, 217202 (2008).
[16] D. Khomskii, Physics **2**, 20 (2009).
[17] R. A. Ewings, A. T. Boothroyd, D. F. McMorrow, D. Mannix, H. C. Walker, and B. M. R. Wanklyn, Phys. Rev. B **77**, 104415 (2008).
[18] U. Staub, Y. Bodenthin, M. García-Fernández, R. A. de Souza, M. Garganourakis, E. I. Golovenchits, V. A. Sanina, and S. G. Luschnikov, Phys. Rev. B **81**, 144401 (2010).
[19] G. Beutier, A. Bombardi, C. Vecchini, P. G. Radaelli, S. Park, S.-W. Cheong, and L. C. Chapon, Phys. Rev. B **77**, 172408 (2008).
[20] J. Okamoto, D. J. Huang, C.-Y. Mou, K. S. Chao, H.-J. Lin, S. Park, S.-W. Cheong, and C. T. Chen, Phys. Rev. Lett. **98**, 157202 (2007).
[21] T. A. W. Beale, S. B. Wilkins, R. D. Johnson, S. R. Bland, Y. Joly, T. R. Forrest, D. F. McMorrow, F. Yakhou, D. Prabhakaran, A. T. Boothroyd, and P. D. Hatton, Phys. Rev. Lett. **105**, 087203 (2010).
[22] J. Koo, C. Song, S. Ji, J.-S. Lee, J. Park, T.-H. Jang, C.-H. Yang, J.-H. Park, Y. H. Jeong, K.-B. Lee, T. Y. Koo, Y. J. Park, J.-Y. Kim, D. Wermeille, A. I. Goldman, G. Srajer, S. Park, and S.-W. Cheong, Phys. Rev. Lett. **99**, 197601 (2007).
[23] R. D. Johnson, S. R. Bland, C. Mazzoli, T. A. W. Beale, C.-H. Du, C. Detlefs, S. B. Wilkins, and P. D. Hatton, Phys. Rev. B **78**, 104407 (2008).
[24] S. Partzsch, S. B. Wilkins, J. P. Hill, E. Schierle, E. Weschke, D. Souptel, B. Büchner, and J. Geck, Phys. Rev. Lett. **107**, 057201 (2011).
[25] H. Jang, J.-S. Lee, K.-T. Ko, W.-S. Noh, T. Y. Koo, J.-Y. Kim, K.-B. Lee, J.-H. Park, C. L. Zhang, S. B. Kim, and S.-W. Cheong, Phys. Rev. Lett. **106**, 047203 (2011).
[26] R. Valdés Aguilar, A. B. Sushkov, S. Park, S.-W. Cheong, and H. D. Drew, Phys. Rev. B **74**, 184404 (2006).
[27] U. Staub, V. Scagnoli, Y. Bodenthin, M. García-Fernández, R. Wetter, A. M. Mulders, H. Grimmer, and M. Horisberger, J. of Synchrotron. Radiat. **15**, 469 (2008).
[28] U. Flechsig, F. Nolting, A. F. Rodríguez, J. Krempaský, C. Quitmann, T. Schmidt, S. Spielmann, and D. Zimoch, AIP Conf. Proc. **1234**, 319 (2010).
[29] U. Staub, V. Scagnoli, A. M. Mulders, K. Katsumata, Z. Honda, H. Grimmer, M. Horisberger, and J. M. Tonnerre, Phys. Rev. B **71**, 214421 (2005).
[30] H. Kimura, Y. Kamada, Y. Noda, K. Kaneko, N. Metoki, and K. Kohn, J. Phys. Soc. Jpn **75**, 113701 (2006).
[31] S. Kobayashi, T. Osawa, H. Kimura, Y. Noda, I. Kagomiya, and K. Kohn, J. Phys. Soc. Jpn **73**, 1031 (2004).
[32] S. Lovesey, E. Balcar, K. Knight, and J. Fernández Rodríguez, Phys. Rep. **411**, 233 (2005).
[33] M. García-Fernández, V. Scagnoli, U. Staub, A. M. Mulders, M. Janousch, Y. Bodenthin, D. Meister, B. D. Patterson, A. Mirone, Y. Tanaka, T. Nakamura, S. Grenier, Y. Huang, and K. Conder, Phys. Rev. B **78**, 054424 (2008).
[34] B. Roessli, P. Fischer, P. Brown, M. Janoschek, D. Sheptyakov, S. Gvasaliya, B. Ouladdiaf, O. Zaharko, E. Golovenchits, and V. Sanina, J. Phys.: Condens. Matter **20**, 485216 (2008).
[35] G. van der Laan, R. V. Chopdekar, Y. Suzuki, and E. Arenholz, Phys. Rev. Lett. **105**, 067405 (2010).
[36] V. Scagnoli and S. W. Lovesey, Phys. Rev. B **79**, 035111 (2009).

[37] A. M. Mulders, S. M. Lawrence, A. J. Princep, U. Staub, Y. Bodenthin, M. García-Fernández, M. Garganourakis, J. Hester, R. Macquart, and C. D. Ling, Phys. Rev. B **81**, 092405 (2010).
[38] E. Schierle, V. Soltwisch, D. Schmitz, R. Feyerherm, A. Maljuk, F. Yokaichiya, D. N. Argyriou, and E. Weschke, Phys. Rev. Lett. **105**, 167207 (2010).
[39] J. C. Lang, D. R. Lee, D. Haskel, and G. Srajer, J. Appl. Phys. **95**, 6537 (2004).
[40] P. G. Radaelli and L. C. Chapon, J. Phys.: Condens. Matter **20**, 434213 (2008).
[41] K. M. D. Hals, Y. Tserkovnyak, and A. Brataas, Phys. Rev. Lett. **106**, 107206 (2011).